Paper:

Adaptive Gait for Large Rough Terrain of a Leg-Wheel Robot (Third Report: Step-Down Gait)

Shuro Nakajima and Eiji Nakano

The Department of Advanced Robotics, Chiba Institute of Technology
2-17-1 Tsudanuma, Narashino, Chiba 275-0016, Japan
E-mail: shuro.nakajima@it-chiba.ac.jp
[Received April 4, 2008; accepted April 4, 2008]

A leg-wheel robot has mechanically separated four legs and two wheels, and it performs high mobility and stability on rough terrains. The adaptive gait for large rough terrains of the leg-wheel robot is composed of three gait strategies. In this paper, the step-down gait, which is one part of the adaptive gait, is described. The point of the flow of the step-down gait is described. When the robot approaches a downward step, a forefoot touches the surface deeply. It forecasts the existence of the downward step by the information on the forefoot's touch point. After that, the robot does the step edge searching operation. This searching operation is the point for going down the step, since the robot fell under the step if it has walked without knowing the step. When the body goes down the step a little, the load sharing ratio of legs increases so that the load of the body rests upon legs. Therefore, the robot finds the edge of it, and it changes footsteps for preparation of going down the step. After the preparation, it can lower the body from the step supported by all legs and wheels. To lower the body, the following items are needed similar to the case of an upward step: 1. Acquisition of target value of lowering the body. 2. Correspondence to difference between target depth and actual depth.[1]

Keywords: mobile robot, leg-wheel robot, adaptive gait, rough terrain, motion control

1. Introduction

Legs, which enable robots to make arbitrary and irregular contacts with the ground, can stably traverse a wide range of terrain including steps and slopes with stability. Legs are mechanically complex, however, positioning and leg control rely on recognition of the external environment, leaving a lot of tasks to solve for practical use.

We have been studying separated leg-wheel robots with 4 legs, two on the front side and two on the back side, each having 3 degrees of freedom (DOF), and with 2 independent wheels, one on each side, to enable robots to traverse on unknown rough terrain but requiring less accuracy in recognition of the external environment and simpler control to make the robot practical [1, 2] (**Fig. 1**). We propose basic movement control [1] for rough terrain with unevenness within ± 0.1 m (regular rough terrain) without the need for environment recognition sensors. Basic movement control does not cover all rough terrain since much is more uneven than regular rough terrain.

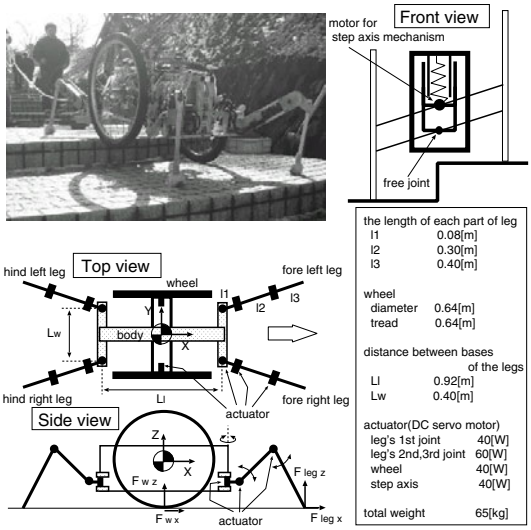

Fig. 1. A leg-wheel robot "Chariot 3".

We proposed 3 gait strategies for large rough terrain by classifying such terrain for leg wheel robots to traverse [3]. We proposed step-up gait control [4] targeting rough terrain with ascending steps of 0.1-0.2 m. This study targets step-down gait for descending steps of 0.1-0.2 m in rough terrain and describes control and movement ability for it.

The gait strategy Ohmichi et al. proposed for similar leg-wheel robots [5] was not targeted at unknown rough terrain. We target unknown rough terrain for leg-wheel robots in this study.

Conventional 4- and 6-leg-robots realized movement for rough terrain by force control using accurate force information from legs [6–9], but we propose movement control for unknown rough terrain using only internal sensors, i.e., angle sensors for individual joints and positioning (pitch and roll) of the robot. We do not used external sensors because they are less accurate in natural environments such as slopes, steps, weedy or muddy land,

1. This paper is the full translation from the transactions of JSME Vol.72, No.721.

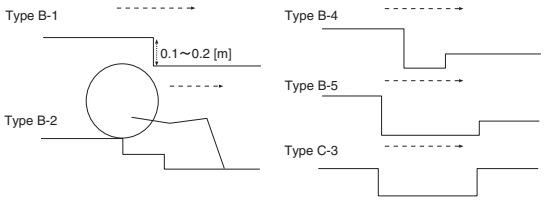

Fig. 2. Targeted rough terrain of the step-down gait.

and snow, with possible errors due to noise and other factors. Our research policy holds that, for practical application, robots traversing unknown rough terrain should move based on information from internal sensors alone and that external sensors should be used to further enhance the capability.

2. Step-Down Gait Flow

Figure 2 shows our targeted large rough terrain. Type B-1 is a single descending step of 0.1-0.2 m. Type B-2 is a double step with the middle located between the front leg contacts and wheel contacts. Type B-4 and B-5 steps have grooves in the middle. Finally, type C-3 is a planar terrain with a groove. The types B-4 and type B-5 differ in whether the wheel drops into the groove, and the groove of type C-3 has a length for the wheels to drop into it. Since classification and selection of the terrains were described previously [3], we do not detail them in this paper. As in the studies [3, 4], steps are made up of planes.

We targeted a gait where the robot is supported by all 4 legs and wheels when lowering the body itself to descend steps. It is desirable for the wheels to continuously contact the ground and support the robot to ensure stability, energy saving, distributed drive force and loads, which are the same as in the step-up gait [4]. We call the gait supported by all 4 legs and wheels "all-leg-support gait."

Since we use the all-leg-support gait to traverse large rough terrain as mentioned above, we exclude large steps in which the robot would take more than one stride to descend the step. The stride used in this study is 0.35 m, which is wide enough to let the robot traverse uneven terrain within 0.2 m (because the stride required to traverse a 0.2 m step is 0.297 m).

Figure 3 shows flow of the step-down gait. For regular rough terrain, the robot is driven by basic movement control [1] using trot gait [2] for legs, which is called the normal gait (**Fig. 3(a)**).

When a front leg contacts a lower face of a step, the robot assumes the existence of the step and estimates the height using the positioning information of the front leg and the inclination of the robot [4] (**Fig. 3(b)**). The robot does not know where the descending step starts from. Upon detecting a descending step, the robot starts searching for the edge of the descending step (**Fig. 3(c)**-(**h**)).

During the searching motion, the robot moves forward supported by all 4 legs and wheels and it repositions all legs at the start positions in the leg movable ranges every time after it moves by one stride. Since the front leg

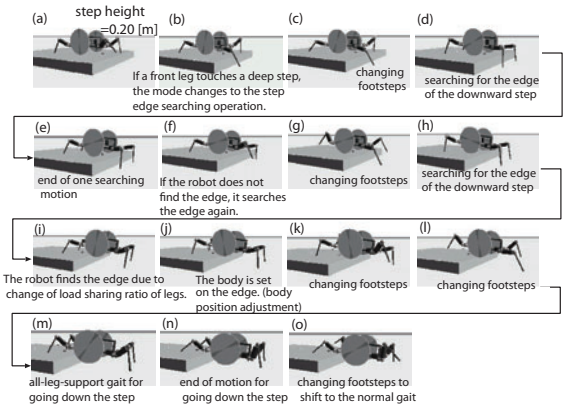

Fig. 3. Flow of the step-down gait.

contacts and wheel contacts differ in location, the robot does not necessarily detect the edge of the descending step by one stride. After repositioning the legs, the robot normally repeats the searching motion. In the cases of grooves, however, the legs may be positioned out of the groove after the first searching motion and the robot may not detect the descending step. To address the problem, the robot retains the front leg height information for the difference between the front leg contacts and wheel contacts and uses the lowest value to assess the step. During the searching motion for the edge of a descending step, when the robot starts descending the step, the load on the legs will increase thus increasing leg load sharing ratio k_{leg} (**Fig. 3(i)**). Leg load sharing ratio k_{leg} represents the ratio of the weight supported by legs to the entire weight of the robot (Eq. (1)).

$$k_{\text{leg}} = \frac{\sum_{i=1}^{n}(\delta_{zi}/C_{zi})}{W} \quad \ldots\ldots\ldots\ldots (1)$$

where n represents the number of support legs, δ_i the deviation of actual positions of support legs from the targets in the direction of the z axis of the body coordinates ([actual position]−[target position]), C_{zi} the compliance of support leg i in the direction of the z axis, W the weight of the robot. Making use of the characteristics of k_{leg}, the edges of descending steps are detected by monitoring changes of k_{leg} during the searching motion for the edges of descending steps.

Upon detection of an edge by the searching motion, the center of gravity (COG) of the body should be slightly beyond the edge (**Fig. 3(i)**). For this, the robot needs to pull the body back slightly to position the COG on the edge, which is called "body position adjustment" (**Fig. 3(j)**). This motion is needed to stabilize the robot for leg repositioning (preparatory leg repositioning, **Fig. 3(k)**, **(l)**) to make stride widths maximum.

Upon position adjustment of the COG on the edge, the robot starts descending in the all-leg-support gait (**Fig. 3(m)**, **(n)**). It is difficult for the robot to determine whether descending has been completed under circumstances where accurate topography information is not available. For this, it is desirable to secure the maximum stride widths in all-leg-support gait. After that, the robot advances the body in the all-leg-support gait un-

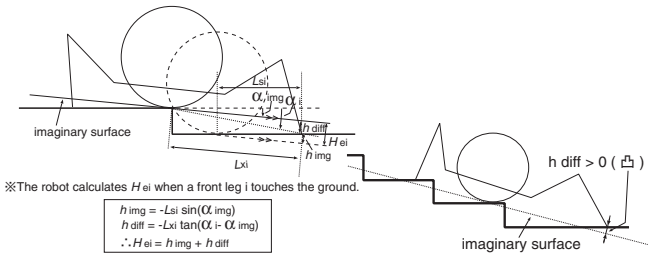

Fig. 4. Estimation of a step depth.

Fig. 5. Consecutive downward steps.

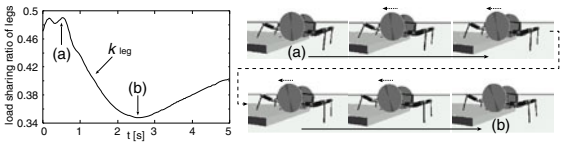

Fig. 6. Load sharing ratio of legs during the body position adjustment.

til the legs reach the movable limits, and then the robot changes the gait to the normal gait (terminating leg repositioning, **Fig. 3(o)**).

3. Step-Down Gait Control

3.1. Detection of Descending Step

The descending step is assessed using estimated step height H_{ei} for front leg i, which is the height from the imaginary surface (**Fig. 4**) in the vertical direction. Since H_{ei} is detailed in another paper [4], it is not described here.

The estimated height H_{ei} of front leg i can be divided into h_{diff}, attributable to the difference from the imaginary surface, and h_{img}, attributable to the imaginary inclination [1] (the inclination of the imaginary surface). Since H_{ei} includes h_{img} from the imaginary inclination, H_{ei} will be calculated negative even for flat descending slopes. Judgment simply based on H_{ei} would cause the robot to erroneously detect a flat descending slope as a descending step. To avoid this, h_{diff} is included in the evaluation as described below.

As for the threshold for judgment, we used 2 different values by the following cases. The values were determined experimentally.

Normal case (Case 1): With the condition that h_{diff} is -0.02 m or less to avoid erroneous detection for flat descending slope, when H_{ei} is -0.10 m or less, the robot determines that it is descending step in large rough terrain.

Terminating repositioning case (Case 2): In the case of successive steps (**Fig. 5**), the h_{diff} will be larger for the last step than that of normal cases. This makes h_{diff} positive and H_{ei} larger, causing possible failure of detecting descending steps. To avoid this situation, only condition that H_{ei} is -0.05 m or less is used for detecting descending steps during the terminating repositioning period.

3.2. Searching Motion for Edge of Descending Step

Upon detection of a descending step, the robot repositions all legs to their start position in their movable ranges, and starts the searching motion for the edge of the descending step. During the searching motion, the robot advances the body by monitoring the leg load sharing ratio from the start to end position in the leg movable ranges.

When the body goes beyond the edge of the descending step, the leg load sharing ratio k_{leg} will increase. The detection of the edge is based on this characteristic. Specifically, the robot determines the edge when k_{leg} becomes larger by $D_{\text{ratio}} = 0.1$ (experimentally determined) compared to a minimum value during the searching motion (**Fig. 11(c)**, **(6)**).

Since the body position is slightly beyond the edge when it has detected the edge, the robot needs to pull the body back onto the edge (body position adjustment). When having detected the edge immediately after the start of the searching motion (within 0.05 m) and the step height is 0.2 m or less, the robot does not conduct the body position adjustment because enough stride widths are available without the body position adjustment.

3.3. Body Position Adjustment

When the robot has detected the edge of a descending step, the position of the body is slightly beyond the edge (**Fig. 6(a)**). Repositioning of the legs may cause the body to fall from the step. To avoid this, body position adjustment is needed to pull the COG of the body back on the edge. This movement is conducted supported by all legs, so it is stable. The right pictures in **Fig. 6** show a series of movement of this (0.3 s intervals). When the robot has detected (**Fig. 6(a)**) the edge of a descending step, the COG of the body is pulled onto the edge (**Fig. 6(b)**). The left graph in **Fig. 6** shows transition of leg load sharing ratio k_{leg}. This data was measured with a step of 0.15 m moving the body backward over the edge. The moving speed was 0.06 m/s (determined experimentally). This figure indicates the following three characteristics of leg load sharing ratio k_{leg} during the body position adjustment.

1. k_{leg} decreases from (a) to (b).
2. The pace of change decreases around (b).
3. k_{leg} becomes minimum around (b) and then increases.

During the body position adjustment, when one of the above characteristics appears, the robot determines that the COG of the body has been pulled back on the edge and terminates the adjustment. The criteria were experimentally determined. For case 1: when k_{leg} decreases by 0.13 or more. For case 2: when the pace of change is 0.067 or less per second during 0.9 s periods. For case 3, when the increase from the minimum is 0.04 or more.

3.4. All-Leg-Support Gait Control

After the body position adjustment, the body is supported by all 4 legs and both wheels and descends the step in the all-leg-support gait.

It starts from a state in which all legs have been repositioned to their start positions in their movable ranges, then, the robot descends the step in the all-leg-support

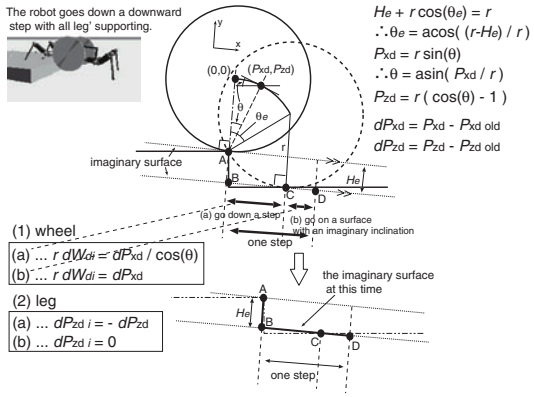

Fig. 7. Wheel and leg control when going down a step with all legs' supporting.

state, and ends up when the legs have reached to their movable limits. As in the case of step-up gait [4], when front leg i contacts the ground in leg repositioning, the robot obtains estimated step height H_{ei} of front leg i. The robot employs the average of the estimated heights of the left and right front legs as the estimated step height H_e.

3.4.1. Wheel Control

Figure 7 shows wheel movement during the all-leg-support gait. The robot descends the step during the first half of one stride in the all-leg-support gait (A→C), and then moves forward (C→D). The imaginary surface for one stride at the beginning of the all-leg-support gait passes though points A-D. When we assume that robot pitch angles are controlled to be parallel to the imaginary surface so that the robot travels in the direction parallel to the surface, the rotation angle for infinitesimal time dW_{di} is expressed by Eq. (2) using dP_{xd} for the distance change of the center of the wheel for infinitesimal time in the direction of x axis of the body coordinates, r for the radius of the wheels, and θ for the rotation angle from the start point of the all-leg-support gait. Proportional-derivative (PD) control is employed to follow the target wheel angles. The reason for controlling the body pitch angle parallel to the imaginary surfaces is to provide larger leg movable ranges for the front and back legs both in support and swing phases, as in the case of the normal gait [1].

$$\begin{cases} dW_{di} = dP_{\mathrm{xd}}/(r\cos\theta) & ((\mathrm{a})\ \theta < \theta_e) \\ dW_{di} = dP_{\mathrm{xd}}/r & ((\mathrm{b})\ \theta \geq \theta_e) \end{cases} \quad . \quad . \quad (2)$$

When the center of the wheel is (P_{xd}, P_{zd}) in the body coordinates at the start point of the all-leg-support gait, θ is obtained as shown in **Fig. 7**, where θ_e represents the angle, between the line segment from the wheel center to point A when descended the step and the line segment from point A perpendicular to the imaginary surfaces. dP_{xd} is given as a command.

As the robot moves toward point D, imaginary and actual surfaces deviate. The deviation, however, is at most 0.003 m with a step of 0.1 m in which the distance CD becomes maximum thus giving the maximum deviation. The error is acceptable because it can be absorbed by leg compliance and wheel suspension.

3.4.2. Leg Control

Leg trajectories are determined geometrically in relation to the center of wheel (P_{xd}, P_{zd}) as in the case of the wheels. To lower the body, legs need to be lifted. Leg trajectory is obtained from **Fig. 7** as follows:

$$\begin{cases} dP_{\mathrm{zd}\,i} = -dP_{\mathrm{zd}} & ((\mathrm{a})\ \theta < \theta_e) \\ dP_{\mathrm{zd}\,i} = 0 & ((\mathrm{b})\ \theta \geq \theta_e) \end{cases} \quad . \quad . \quad . \quad . \quad . \quad (3)$$

where dP_{zd} represents the distance change of the center of the wheel for infinitesimal time in the direction of the z axis of the body coordinates and $dP_{\mathrm{zd}\,i}$ represents that of leg i.

The leg position in the direction of x and y in body coordinates is determined by a gait algorithm previously proposed [2].

In addition to Eq. (3), since legs contact the ground discretely, we need an initial value for target leg contact positions. To absorb various disturbances from terrain surfaces by leg compliance as in the normal gait, the targeted leg height when switching from swing to support phases is assigned to be lower than the actual height by Δ_s, the basic setting [1]. Leg compliance is set as in the normal gait [1] and leg trajectory is adjusted at the same timing as in the normal gait so that the body pitch angle keeps parallel to the imaginary surfaces in the all-leg-support gait.

3.4.3. Step Axis Control

As in the step-up gait [4], feedback control is implemented by Eq. (4) based on the sky-hook damper theory so that the targeted body roll angle $\theta_{\mathrm{d}r}$ becomes 0 for better stability. The body roll angle is controlled by the motor on a step axis mechanism (upper right in **Fig. 1**).

$$\begin{aligned} T_{\theta_r} &= -K_r(\theta_r - \theta_{\mathrm{d}r}) - D_r(\dot{\theta}_r - \dot{\theta}_{\mathrm{d}r}) \\ &= -K_r\theta_r - D_r\dot{\theta}_r. \quad . \quad . \quad . \quad . \quad . \quad . \quad . \quad . \quad . \quad . \quad . \quad . \quad (4) \end{aligned}$$

T_{θ_r} represents the torque of the motor on the step axis, θ_r the body roll angle, $\theta_{\mathrm{d}r}$ the target body roll angle, K_r the angle gain, and D_r angular velocity gain.

As in the step-up gait, when entering a descending step diagonally, this mechanism enables the robot to lower the left and right wheels in different timing while keeping the body roll angle horizontal.

3.4.4. Measures for Over-Estimated Step Height

Since the front leg contact differs from a step location, estimated step height H_e may not be accurate depending on topography. A double step, for example, step height H_e estimated at the beginning of the all-leg-support gait will be larger than the actual height for the robot to descend first (**Fig. 8**).

Small error in estimated step height H_e is absorbed by leg compliance and wheel suspension, but not error that is large.

With over-estimated height in all-leg-support gait, the robot would lift the legs excessively causing the legs detached from the ground, making the robot unstable (**Fig. 8**). In this case, it will be observed as a phenomenon

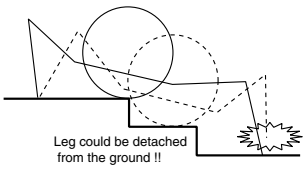

Fig. 8. A double step.

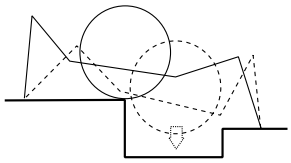

Fig. 9. A concave terrain.

of decrease in leg load sharing ratio k_{leg} due to reduced loads on legs. To address this problem, we introduced an algorithm to monitor k_{leg} when lowering the body in the all-leg-support gait and to stop lifting legs when k_{leg} goes beyond threshold $R_{\text{down}} = 0.3$ (the value experimentally determined). The control of wheel is also changed from (a) to (b) in Eq. (2).

3.4.5. Measures for Under-Estimated Step Height

With topography in **Fig. 9**, step height H_e estimated at the beginning of the all-leg-support gait will be smaller than the actual height for the robot to descend. If the estimation error is large, the wheels would not come in contact with the ground even after the completion of all-leg-support gait.

If legs were repositioned in this condition, the body would decline largely losing stability. To avoid this, we introduced an algorithm to monitor the leg load sharing ratio k_{leg} to see whether the wheels contact the ground. If it is determined no contact, the body will be further lowered. This algorithm is activated after the first descent throughout the all-leg-support gait. Specifically, if k_{leg} exceeds threshold $k_{s\text{down}} = 0.6$, the robot lowers the body until the wheels contact the ground for the period (from the point when the body has been lowered in all-leg-support gait (at the end of (a) in **Fig. 7**) until the completion of the all-leg-support gait (at the end of (b) in **Fig. 7**). As in the step-up gait, the judgment is made only if the condition meets over a certain percentage of predetermined time to avoid false judgment.

4. Simulation and Experiments of Type B-1

We verify in this section that the proposed gait enables a robot to traverse the targeted large rough terrain.

Simulation and experimental conditions were as follows: swing leg speed was 0.5 m/s, swing leg lifting height 0.2 m, maximum leg lowering for a swing leg to land 0.4 m, stride width 0.35 m, basic deviation of actual leg locations from targets $\Delta_s = 0.043$ m, stiffness for all legs and for suspension in the direction of the z axis 7500 N/m, the basic load sharing ratio between legs and wheels 1:1, P and D gains for wheel rotation control 80 Nm/rad and 20 Nm/rad/s, and P and D gains for step axis control 1000 Nm/rad and 100 Nm/rad/s. The gait was a trot [2] and the environment was assumed to be unknown. We used the Open Dynamics Engine (ODE) to dynamically simulate assuming rigid contact between the legs and ground and the wheel and ground. The friction coefficient between the legs and ground was set at 0.4 and

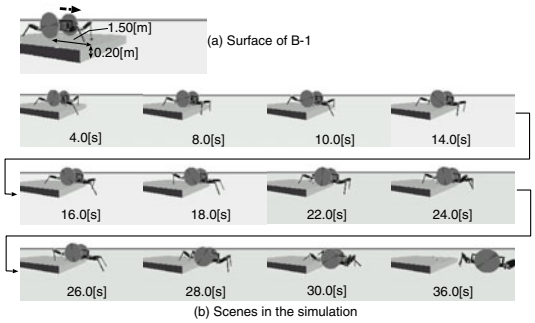

Fig. 10. Scenes in the simulation (Type B-1 terrain).

that between the wheels and ground at 0.7.

4.1. Simulation (Type B-1)

Simulation was made with an unknown descending step of 0.20 m (**Fig. 10(a)**). **Fig. 10(b)** shows the results demonstrating successful traversing over the step and **Figs. 11(a)**-**(f)** show the data. **Fig. 11(a)** shows robot target translational velocities. Small fluctuations in target velocities result from restrictions on velocity commands activated by event-driven control [2]. Periods (1) in the figure correspond to stops of the robot for leg repositioning. Periods (2) correspond to searching motions for the edge of the descending step. We see that the robot could not find the edge for the first time and made several attempts to detect it. Period (3) corresponds to a body position adjustment after the detection of the edge of the descending step. Note that the velocities are negative showing backward movement of the body. Then, in period (4), the robot descended the step in the all-leg-support gait. The estimated step height was $H_e = -0.180$. For reference, theoretical H_e value for steps of 0.20 m is -0.181 m.

Figure 11(b) shows transition of the body pitch and roll angles and the inclination of the imaginary surfaces [1]. Positive body pitch angles represent front down and negative front up. Positive body roll angles represent left up and negative right up. The figure demonstrates that the body pitch angle followed the imaginary inclination and the body roll angles were kept horizontal.

Figure 11(c) shows the transition of leg load sharing ratio k_{leg} for the period of 17.5 to 23.0 s. In this period, the robot was making the third searching motion and body position adjustment. A series of pictures on the right was taken at intervals of 1.0 s. Leg load sharing ratio k_{leg} in period (5) showed decreasing tendency. This is because the robot supposed positive imaginary inclination (i.e., front down) until it reached the descending step, so body positioning is adjusted for a descending slope. The actual surface is horizontal, however, so the body is ascending against the imaginary surface, resulting in increasing load sharing by the wheels or lower k_{leg}. k_{leg} increases in period (6) are attributable to increasing leg support so that the body does not drop from the step after its passing the edge of the step. The edges of the descending step are detected when the positive change of k_{leg} exceeds threshold $D_{\text{ratio}} = 0.1$. Upon detection of the edge by the searching motion, the robot stopped and started a body position ad-

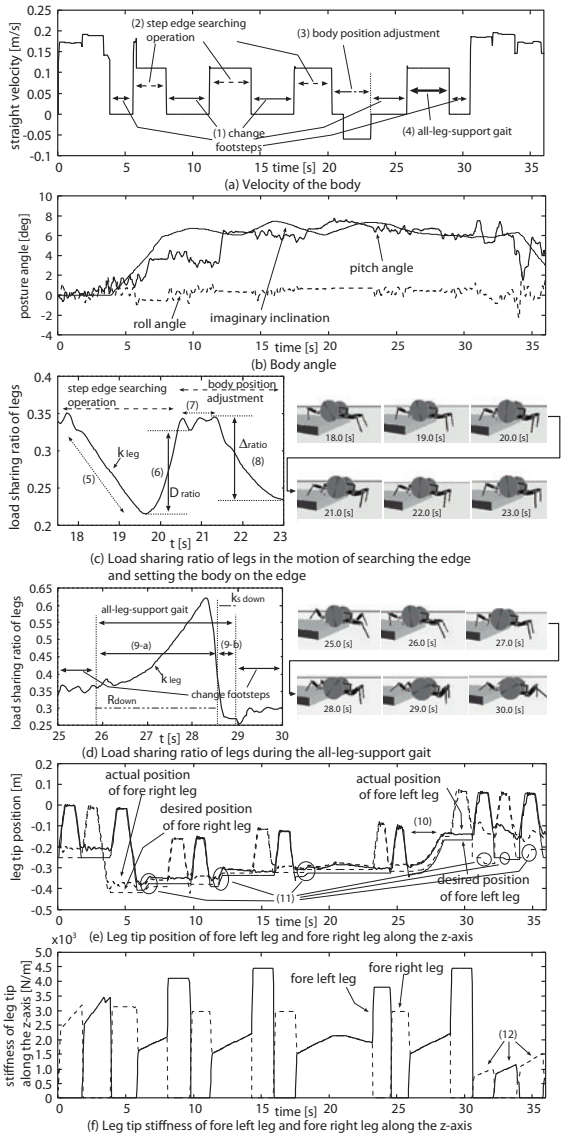

Fig. 11. Simulation data (Type B-1 terrain).

justment in period (7). k_{leg} decreased in period (8). This is attributable to increased loads on wheels as the body was pulled back onto the upper face of the step by the body position adjustment. Then, the robot finished the body position adjustment when the change exceeded threshold $\Delta_{\text{ratio}} = 0.13$ (corresponding to (a) through (b) in the left graph in **Fig. 6**).

Figure 11(d) shows the transition of leg load sharing ratio k_{leg} for the period of 25 to 30 s. A series of pictures on the right was taken at intervals of 1.0 s. During period (9-a) in which the body was lowered, the robot compared the leg load sharing ratio k_{leg} to threshold R_{down} to respond to possible cases of over-estimation of step height, which was no problem in this case. After body lowering, the robot compared k_{leg} to threshold $k_{s\text{down}}$ to respond to possible cases of under-estimation of step height where body lowering would be insufficient, which was no problem in this case (during period (9-b) in **Fig. 11(d)**).

Figure 11(e) shows the target and actual front (right and left) leg positions in the direction of the z axis in body coordinates. At period (10) in the figure in the all-leg-support gait, the target positions for the legs were raised to lower the body. As in the normal gait [1], trajectories for legs were adjusted in periods (11) to make the body pitch angle parallel to the imaginary inclination after leg landing. Deviation between target and actual positions is caused by compliance.

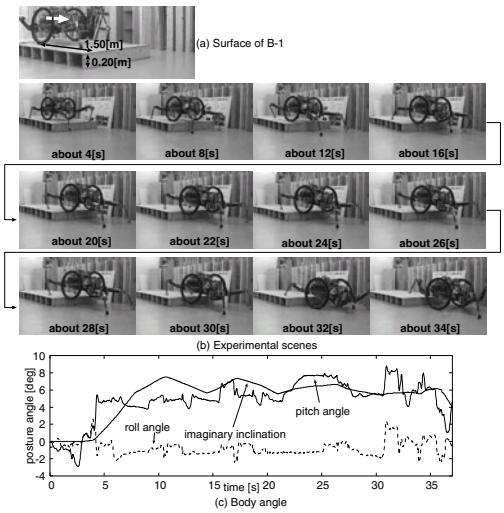

Fig. 12. Experimental scenes (Type B-1 terrain).

Figure 11(f) shows stiffness of the left and right front legs in supporting phases. The leg stiffness in swing phases is displayed as 0 for simplicity in graph. During the searching motion for the edge of the descending step, body position adjustment, and all-leg-support gait, the stiffness decreased because the robot was supported in all-leg-support gait with the positional deviations of legs maintained at the same value as basic setting Δ_s in the normal gait (2 legs in swing phases). Stiffness became low in period (12). This is because the deviation became larger at the time and the robot was adjusting the leg force.

4.2. Experiments (Type B-1)

Experiments (**Fig. 12(b)**) were conducted with an unknown descending step of 0.2 m (**Fig. 12(a)**). Due to space limitation, only body angle data is shown in **Fig. 12(c)**. The body angles were about the same as those obtained by simulation. The body angles in experiments fluctuated more than in simulation, presumably due to joint friction and modeling errors in the robot. The estimated step height was $H_e = -0.177$. We confirmed that other experimental data matched that obtained by simulation.

5. Traverse Experiments on Other Rough Terrain

This section discusses cases in which the robot moves diagonally toward a step, in which step heights differ laterally, and in which descending steps are slightly slanted, as well as other cases in **Fig. 2**. We confirmed traversal on all terrain by both simulation and experiments. Due to space limitation, we summarize experiments below.

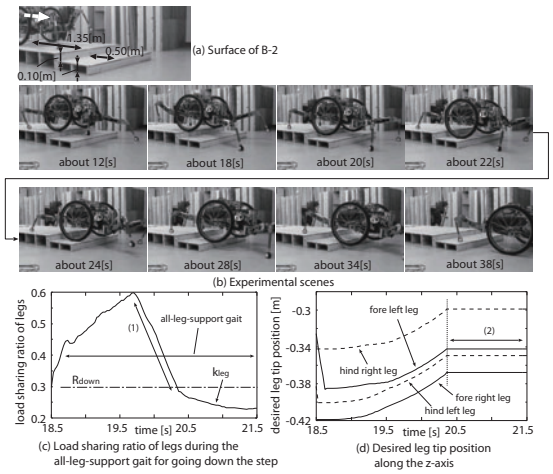

Fig. 13. Type B-2 terrain.

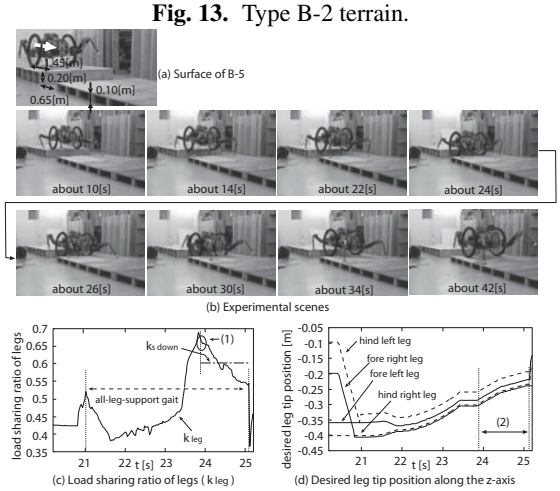

Fig. 14. Type B-5 terrain.

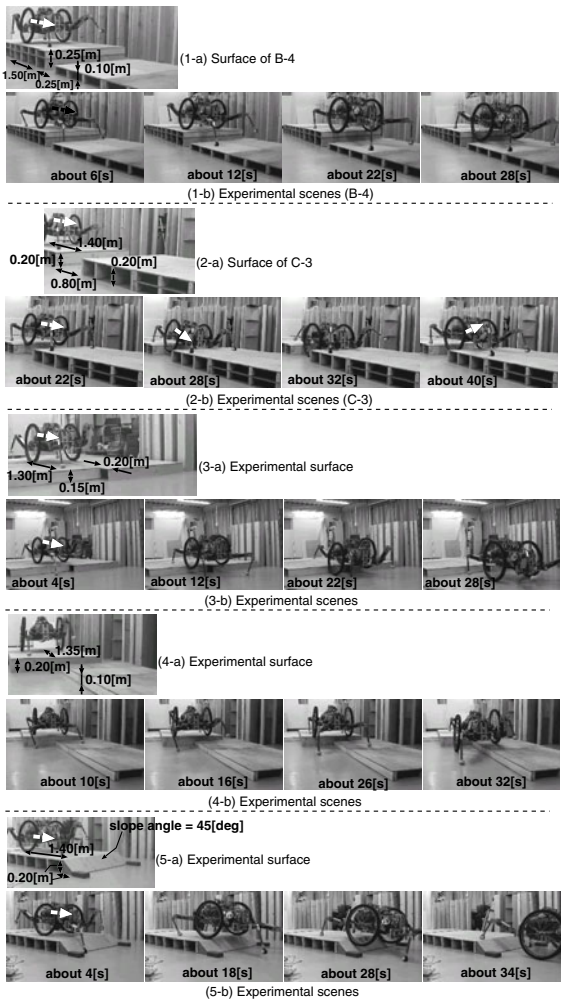

Fig. 15. Other rough terrains.

5.1. Type B-2 Terrain

Experiments (**Fig. 13(b)**) were conducted with an unknown descending double step, each 0.10 m high (**Fig. 13(a)**). The estimated step height was larger than the actual height for the body to descend, so the legs and wheels were controlled in the above-mentioned algorithm for step height over-estimation. The estimated heights were $H_e = -0.162$ m for the first step and $H_e = -0.078$ m for the second step.

Figure 13(c) shows the transition of leg load sharing ratio k_{leg} during a period of descending the first step in all-leg-support gait. Compared to the actual height of -0.1 m, the estimated height was $H_e = -0.162$ causing excessive leg lifting. This reduces k_{leg} in period (1) in the figure down below threshold R_{down}. As a result, the robot stopped lowering the body by keeping the leg at the same height in the z direction in period (2) in **Fig. 13(d)**.

5.2. Type B-5 Terrain

Experiments (**Fig. 14(b)**) were conducted with a descending step followed by a groove of 0.65 m in width (**Fig. 14(a)**). The estimated step height in all-leg-support gait was $H_e = -0.083$. The characteristic of the B-5 terrain is that the front leg contacted the face of -0.1 m in height in all-leg-support gait, while the height of the bottom face of the groove to which the body needed to be lowered was -0.2 m. Upon completion of body lowering, the body was not sufficiently lowered due to under estimation of the step height, which activated the algorithm for under estimation to further lower the body down to the surface of -0.2 m.

Figure 14(c) shows the transition of leg load sharing ratio k_{leg}. The robot detected insufficient lowering at time (1) and lowered the body further more. **Fig. 14(d)** shows the target front leg positions in the direction of the z axis. Period (2) corresponds to body lowering as the countermeasure of under estimation of the descending step, which was activated by detection at time (1) in **Fig. 14(c)**.

5.3. Type B-4 Terrain

Figure 15(1-b) shows experimental results with a descending step (**Fig. 15(1-a)**), in which a groove of 0.25 m in length is located after the step. Since the wheels are bigger than the groove and did not dropped into it, the robot traversed as in the Type B-1 terrain.

5.4. Type C-3 Terrain

Figure 15(2-b) shows experimental results with a descending step (**Fig. 15(2-a)**), where a groove with more length of the wheel diameter is located after the step. The wheels once dropped into the groove but escaped from the groove by step-up gait.

5.5. Diagonal Entrance to Step

When entering a step diagonally, compared to orthogonally, step starting points for the robot differ between left and right sides.

To evaluate this condition, we conducted experiments (**Fig. 15(3-b)**) with a step (**Fig. 15(3-a)**) of 0.15 m having different starting points by 0.2 m between left and right sides. The right wheel descended the step by the step-down gait. Then, the left wheel descended in the normal gait without detecting the step as a descending step, because the body had been lowered by a half.

5.6. Step with Laterally Different Heights

We conducted experiments with a step (**Fig. 15(4-a)**) whose heights differed laterally for the robot (**Fig. 15(4-b)**). The robot traversed the step keeping its body roll angle horizontal using the step axis control even though the step height differed on both sides.

5.7. Slanted Descending Step

We conducted experiments with a slanted descending step (**Figs. 15(5-a)** and **15(5-b)**). The robot traversed the step by absorbing the difference between assumed and actual topography by compliance. We also experimentally confirmed that the robot successfully traversed topography including long diagonal steps by using multiple step-down gaits if the topography provided space for wheels to securely land during the time of leg repositioning.

6. Conclusions

We have proposed control for step-down gait for leg-wheel robots as an adaptive gait for large rough terrain. Traversing was demonstrated by both simulation and experiments on large rough terrain using the proposed gait. Simulation and experiments for all targeted topography confirmed that the proposed gait enabled the robot to successfully traverse terrain (part of results reported due to space limitation). We will continue studying gaits for large rough terrain using the remaining movement strategy (i.e., step-over) to propose and verify its control to be reported in another paper.

References:

[1] S. Nakajima, E. Nakano, and T. Takahashi, "The Motion Control Method for a Leg-wheel Robot on Unexplored Rough Terrains," Journal of the Robotics Society of Japan, Vol.22, No.8, pp. 1082-1092, 2004.

[2] S. Nakajima, E. Nakano, and T. Takahashi, "Trot and Pace Gaits based on the Predictive Event Driven Method for a Leg-wheel Robot," Journal of the Robotics Society of Japan, Vol.22, No.8, pp. 1070-1081, 2004.

[3] S. Nakajima and E. Nakano, "Adaptive Gait for Large Rough Terrain of a Leg-wheel Robot (First Report: Gait Strategy)," Journal of Robotics and Mechatronics, Vol.20, No.5, pp. 801-805, 2008.

[4] S. Nakajima and E. Nakano, "Adaptive Gait for Large Rough Terrain of a Leg-wheel Robot (Second Report: Step-Up Gait)," Journal of Robotics and Mechatronics, Vol.20, No.6, pp. 913-920, 2008.

[5] T. Ohmichi and T. Ibe, "Development of Vehicle with Legs and Wheels," Journal of the Robotics Society of Japan, Vol.2, No.3, pp. 244-251, 1984.

[6] S. M. Song and K. J. Waldron, "Machines That Walk:The Adaptive Suspension Vehicle," MIT Press, 1989.

[7] D. M. Gorinevsky and A. Shneider, "Force Control of Legged Vehicles over Rigid and Soft Surfaces," International Journal of Robotics Research, Vol.9, No.2, pp. 4-23, 1990.

[8] J. E. Bares and W. L. Whittaker, "Configuration of Autonomous Walkers for Extreme Terrain," The International Journal of Robotics Research, Vol.12, No.6, pp. 535-559, 1993.

[9] T. Hori, H. Kobayashi, and K. Inagaki, "Force Control for Hexapod Walking Robot with Torque Observer," Proc. of the Int. Conf. on Intelligent Robots and Systems, pp. 1294-1300, 1994.

Name:
Shuro Nakajima

Affiliation:
Ph.D. (Information Science), Associate Professor, The Department of Advanced Robotics, Chiba Institute of Technology

Qualification:
Professional Engineer (Mechanical Engineering)

Address:
2-17-1 Tsudanuma, Narashino, Chiba 275-0016, Japan

Brief Biographical History:
1997- East Japan Railway Company
2005- Future Robotics Technology Center, Chiba Institute of Technology
2006- The Department of Advanced Robotics, Chiba Institute of Technology

Main Works:
• S. Nakajima and E. Nakano, "Adaptive Gait for a Leg-Wheel Robot Traversing Rough Terrain (Second Report: Step-Up Gait)," Journal of Robotics and Mechatronics, Vol.20, No.6, pp. 913-920, 2008.

Membership in Academic Societies:
• Institute of Electrical and Electronics Engineers (IEEE)
• The Japan Society of Mechanical Engineers (JSME)
• The Robotics Society of Japan (RSJ)
• Japan Society of Kansei Engineering (JSKE)
• The Institute of Professional Engineers, Japan (IPEJ)

Name:
Eiji Nakano

Affiliation:
Doctor of Engineering, Professor, The Department of Advanced Robotics, Chiba Institute of Technology

Address:
2-17-1 Narashino, Chiba 275-0016, Japan

Brief Biographical History:
1970 Graduated, Postgraduate Course of University of Tokyo
1970- Senior Researcher, Mechanical Engineering Laboratory
1987- Professor, Tohoku University
2005- Professor, Chiba Institute of Technology

Main Works:
• E. Nakano et al., "Leg-Wheel Robot: A Futuristic Mobile Platform for Forestry Industry," 1993 IEEE/Tsukuba Industrial Workshop on Advanced Robotics, 1993.

Membership in Academic Societies:
• Robotics Society of Japan (RSJ)
• Japan Society of Mechanical Engineers (JSME)
• Society of Instrument and Control Engineers (SICE)
• Society of Biomechanism (SOBIM)